Chinese Chemical Letters 34 (2023) 108181

Contents lists available at ScienceDirect

Chinese Chemical Letters

journal homepage: www.elsevier.com/locate/cclet

Simultaneous monitoring of the fluorescence and refractive index by surface plasmon coupled emission: A proof-of-concept study

Lin-Tao Xu[a], Kai-Xin Xie[b], Shuo-Hui Cao[a,c], Yu-Hua Weng[a], Min Chen[a], Zhao Li[a], Yao-Qun Li[a,*]

[a] Department of Chemistry and the MOE Key Laboratory of Spectrochemical Analysis & Instrumentation, College of Chemistry and Chemical Engineering, Xiamen University, Xiamen 361005, China
[b] Department of Chemistry, Taiyuan Normal University, Jinzhong 030619, China
[c] Department of Electronic Science, Xiamen University, Xiamen 361005, China

ARTICLE INFO

Article history:
Received 23 September 2022
Revised 16 January 2023
Accepted 29 January 2023
Available online 1 February 2023

Keywords:
Fluorescence with refractive index information
Surface plasmon coupled emission
Volatile organic compounds
Dye-encapsulated metal-organic frameworks
All-in-one method

ABSTRACT

Simultaneous acquisition of fluorescence property and refractive index using a single surface plasmon coupled emission (SPCE) measurement has been achieved, thus achieving synchronicity in real time. The SPCE sensor was employed for monitoring the adsorption of volatile organic compounds (VOCs) by dye-encapsulated metal-organic frameworks (Dye@MOFs). Refractive index can reveal surface molecular adsorption and the fluorescence with information on refractive index can provide a comprehensive analysis of the adsorption events of VOCs on the interface. Meantime, the signal intensity can be amplified by combining the responses caused by changes in refractive index and the fluorescence property in parallel. This all-in-one method opens up a route to monitoring multiple processes simultaneously occurring on the interface.

Classical fluorescence-based chemosensors enable sensing by providing a variation in fluorescence property [1,2]. Techniques for measuring refractive index such as surface plasmon resonances can offer additional information on surface molecular adsorption, and thus have been widely explored for sensing applications [3–5]. However, the acquisition of information on refractive index and fluorescence properties typically requires the separate measurements of different technologies [6–8], and it is hard to achieve synchronization in true sense for fast chemical processes. Surface plasmon coupled emission (SPCE) is a novel surface-enhanced fluorescence technique with highly directional emission and unique polarization [9–13]. The fluorescent molecules in the excited state interact strongly with the metal surface plasmon in the near-field range of the smooth metal film. And the excited fluorescent molecules state are coupled with the metal surface plasmon and emit the SPCE signal at the prism side with the wave vector matched angles [13]. SPCE technique has been applied to imaging [14], oxygen sensing [15] and biosensing [16,17]. Fluorescence enhancement by green synthesized plasmon nanoparticles has been achieved and explored for high-performance sensing applications [18–20]. SPCE-based sensors have achieved sensing by changes in fluorescence intensity. However, the emission angle in SPCE that can provide information on the refractive index is usually ignored. Benefiting from the sensitivity of SPCE to fluorescence and refractive index, SPCE is promising to be developed as a convenient tool for investigating multiple processes simultaneously occurring on the interface.

The detection of volatile organic compounds (VOCs) is critical in many fields, including disease diagnosis, and quality control in the food and cosmetics industries [21,22]. Metal-organic frameworks (MOFs) have attracted interest as a potential material for manufacturing chemical sensors in recent years. Due to their large surface area and high porosity, MOFs have been applied in many fields, including catalysis [23], gas storage [24] and chemical separation [25]. The most attractive properties of MOFs are their high surface areas, which results in high gas storage capacity. Various MOF-based vapor sensors have been developed *via* the variations in mass [26], optical property [27] and electrical property [28] when MOFs adsorbed target molecules. Most of the sensors based on luminescent metal-organic frameworks realized detection of VOCs through changes in fluorescence properties such as the energy transfer effect [29,30] and the interaction between VOCs and dyes causing fluorescence quenching or enhancement [31–34].

* Corresponding author.
E-mail address: yaoqunli@xmu.edu.cn (Y.-Q. Li).

https://doi.org/10.1016/j.cclet.2023.108181
1001-8417/

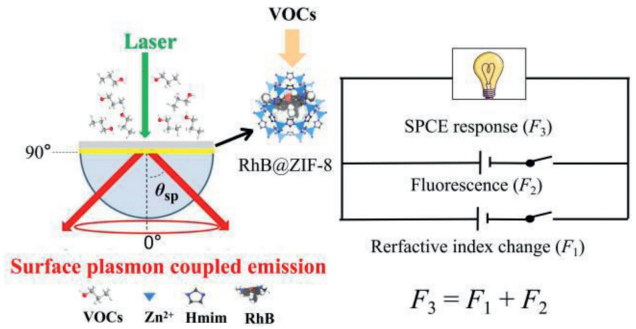

Fig. 1. Experimental setup for SPCE and a schematic representation of RhB@ZIF-8 based SPCE sensor on detecting the VOCs.

During the adsorption of the VOCs, the refractive index changes can provide information about the adsorption of VOCs to MOFs [35–37]. However, there are still no reports on the simultaneous study of refractive index and luminescence property changes during the interaction between VOCs and luminescent metal-organic frameworks.

In this work, angle-scanning SPCE (AS-SPCE) monitors the adsorption of VOCs *in situ*. As shown in Fig. 1, the Reverse Kretschmann (RK) configuration is employed in this study, with an excitation laser and a detector scanning around the prism to obtain angle distribution patterns [38]. Rhodamine B-encapsulated zeolitic imidazolate frameworks (RhB@ZIF-8) film is designed as a dual response material (The synthesis process can be found in Supporting information). The ZIF-8 material serves as an adsorption layer for VOCs, causing a change in refractive index, and the interaction of ZIF-8-encapsulated RhB with VOCs produces a fluorescence response. And the refractive index and fluorescence property of RhB@ZIF-8 material during adsorption is utilized for VOCs detection. The SPCE sensor cleverly measures refractive index and fluorescence property simultaneously by fluorescence signal measurement and combines two signal intensities caused by changes in refractive index and fluorescence property in parallel.

In order to optimize the performance of the RhB@ZIF-8 sensor, we grew RhB@ZIF-8 film on a gold film (the surface roughness of the gold substrate is shown in Fig. S1 in Supporting information), and optimized the thickness of RhB@ZIF-8 film. As shown in Fig. 2A, a p-polarized emission was shown at 51.3° in the first cycle of growth, which meant RhB@ZIF-8 was formed on the gold film. After three growth cycles, the p-polarization (parallel to the incident plane) angle increased to 70°, and an s-polarized emission (perpendicular to the incident plane) appeared at 42.7° (Fig. 2B). To ensure that the synthesis method can produce the desired RhB@ZIF-8 material, we measured the XRD pattern of RhB@ZIF-8 film (Fig. 2C), which were consistent with the reported XRD pattern of ZIF-8 [39,40]. The sharp peaks indicated the high crystallinity of the RhB@ZIF-8 materials. The RhB@ZIF-8 materials were also investigated and identified by the FTIR spectrum (Fig. S2 in Supporting information), the absorption and the fluorescence spectra of the RhB@ZIF-8 materials (Fig. S3 in Supporting information) were characterized. The spectral results indicated the successful encapsulation of the dye molecules in ZIF-8. This formation of RhB@ZIF-8 film was also confirmed by the SEM images for the film grown for three cycles (Fig. 2D). By comparison, we found that after the three growth cycles, the fluorescence intensity of the angle distribution pattern was stronger (Fig. 2B). And the intensity of the s-polarized angle distribution pattern had a greater rate of change for angle shift at the maximum slope θ_{max} (45.3°) (Fig. S4 in Supporting information), which implies a better sensitivity to the change of refractive index [41], so RhB@ZIF-8 grown for three cycles was used as a sensing layer for the VOCs sensor. The thickness and refractive

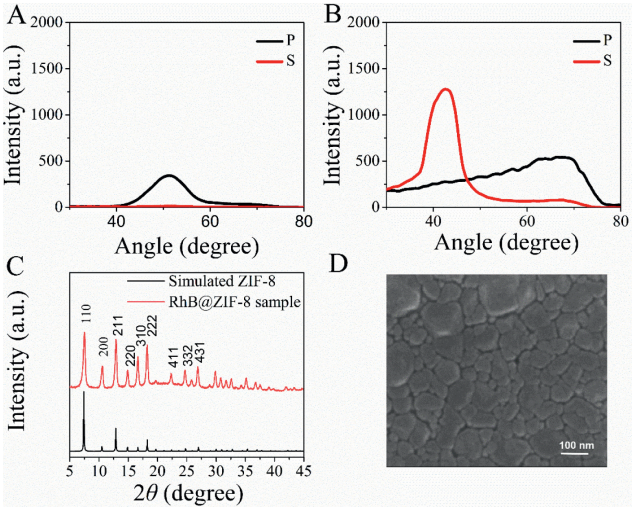

Fig. 2. (A) Angle distribution pattern of RhB@ZIF-8 film grown for one cycle. (B) Angle distribution pattern of RhB@ZIF-8 film grown for three cycles. (C) XRD of RhB@ZIF-8 materials and the simulated one. (D) SEM of RhB@ZIF-8 film grown for three cycles.

index of RhB@ZIF-8 film can be measured by modeling the location of SPCE emission angle(s) with the Winspall software (Figs. S5 and S6 in Supporting information), based on Fresnel equations [42,43] (see details in Section 1 in Supporting information). The optical model can be found in Supporting information. The simulation result indicated the formation of RhB@ZIF-8 film with a thickness of 139 nm and a refractive index of 1.42 on the gold film after three growth cycles.

Isopropanol is very hazardous to human health [22]. Isopropanol vapor was used as the target VOCs to detect the response of the sensor (The process of vapor testing can be found in Supporting information). The solvents were injected into the test chamber without contacting the RhB@ZIF-8 chip (The photograph of the SPCE setup and schematic of the test chamber are shown in Fig. S7 in Supporting information), followed by continuous scanning of the angle distribution pattern until the pattern no longer changed to ensure a balance between adsorption and desorption of the target VOCs on the sensing layer. Fig. 3A showed the performance of the RhB@ZIF-8 based SPCE sensor. After the adsorption of the saturated isopropanol vapor, the angle distribution pattern showed angle shift as well as peak intensity change. The refractive index and thickness of the dielectric over the plasmonic metal film both cause angle shifts in SPCE [44,45]. And it has been reported in the literature that the change in the ZIF-8 thickness is negligible after the adsorption of isopropanol vapor [35]. The VOCs adsorbed by porous ZIF-8 will replace the air in the pores and lead to an increase in refractive index [35,36,46] (Equation details can be found in section 9 in Supporting information), which caused the angle shift. From the theoretical simulation (Fig. 3B), we can derive the refractive index of RhB@ZIF-8 film changed from 1.42 to 1.50 due to the adsorption of isopropanol vapor into the MOF film. It was worth noting that the consistent depth of the simulated reflectivity dips obtained from Fresnel simulations before and after isopropanol vapor adsorption meant the same coupling efficiency with the surface plasmon (Fig. 3B) [47], which implied that the change in peak intensity came from RhB@ZIF-8 materials. To investigate the mechanism of peak intensity change, the response of free space emission was measured under saturated isopropanol vapor. As shown in Fig. 3C, the interaction of the RhB@ZIF-8 materials with isopropanol vapor resulted in a change in the fluorescence property of RhB molecules. The substantial increase in fluorescence intensity was due to the

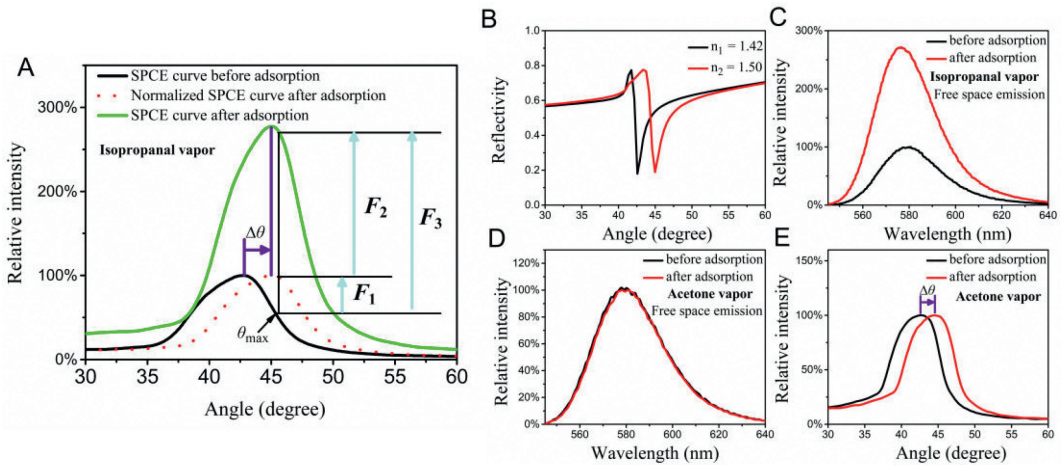

Fig. 3. Mechanism of the RhB@ZIF-8 based SPCE sensor to monitor the adsorption of VOCs. (A) Change of angle distribution pattern recorded at 579 nm light before and after adsorption of saturated isopropanol vapor. (B) Theoretical simulation by Fresnel calculations before and after adsorption of saturated isopropanol vapor. The free space emission spectrum of RhB@ZIF-8 materials before and after adsorption of (C) saturated isopropanol vapor and (D) saturated acetone vapor. (E) Change of angle distribution pattern recorded at 579 nm light before and after adsorption of saturated acetone vapor.

fact that RhB could exist in three different states (lactone, zwitterion, and cation), where the zwitterion showed strong fluorescence. Polar proton solvents (isopropanol) could stabilize the zwitterion and therefore produce an intense fluorescence [32]. The enhancement of free space emission intensity on the sample side was in general agreement with the enhancement of the peak intensity of the angle distribution pattern. During the adsorption of isopropanol vapor, the peak intensity enhancement originated from the change of fluorescence property of RhB@ZIF-8 film. The experimental results suggested that two processes occurred simultaneously in the RhB@ZIF-8 based SPCE sensor during the adsorption of isopropanol vapor: (1) The isopropanol vapor enhanced the fluorescence intensity of RhB molecules; (2) The adsorbed isopropanol vapor changed the refractive index of RhB@ZIF-8 material and caused angle shift. And the same phenomenon occurred during the adsorption of methanol vapor and ethanol vapor (Figs. S9A and B in Supporting information). In our strategy, both processes were monitored simultaneously by a single SPCE signal measurement. To better demonstrate the signal intensity variations caused by refractive index change and fluorescence property change (Fig. 3A), the SPCE curve after adsorption of isopropanol vapor was normalized to show the signal intensity variation caused by refractive index change. The signal intensity variations caused by refractive index change (F_1) can be obtained by measuring the signal change between the red dotted curve and the black curve at θ_{max}. The signal intensity variation caused by fluorescence property change (F_2) can be obtained by measuring the signal change between the green curve and the red dotted curve at θ_{max}. And the SPCE sensor amplified the detection signals (F_3) by combining the signal intensity variations caused by the changes in refractive index (F_1) and the fluorescence intensity (F_2) after the adsorption of VOCs. The reversibility of the sensor was shown in Fig. S8 (Supporting information), the physisorption character of interaction between the isopropanol vapor and the RhB@ZIF-8 materials ensured the reversibility of the sensor. To better demonstrate the performance of the multi-information acquisition sensing strategy, the sensor was used to measure the response to acetone vapor. Conventional fluorescence measurements showed negligible response after adsorption (Fig. 3D). However, the angle shift in fluorescence signal measurement based on SPCE could imply that RhB@ZIF-8 film adsorbed acetone vapor (Fig. 3E). And the same phenomenon occurred during the adsorption of ether vapor and ethyl acetate vapor (Figs. S9C and D in Supporting information). SPCE signal measurement

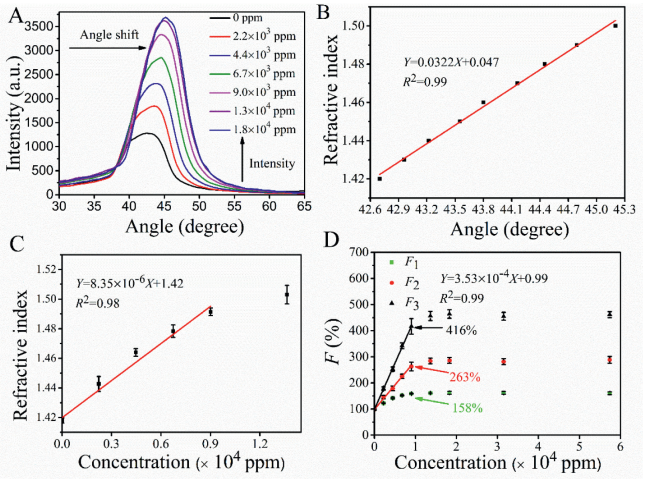

Fig. 4. (A) The angle distribution pattern of the RhB@ZIF-8-SPCE sensor recorded at 579 nm light when exposed to different concentration of isopropanol vapor. (B) Refractive index of RhB@ZIF-8 film as a function of SPCE angle. (C) Dependence of the refractive index of RhB@ZIF-8 film on concentration of isopropanol vapor. (D) The fluorescence intensity variations of the RhB@ZIF-8-SPCE sensor exposed to different concentration of isopropanol vapor.

that acquaints both fluorescence information and refractive index information can provide a comprehensive analysis of the interface compared to traditional fluorescence technique.

To evaluate the sensing performance of the RhB@ZIF-8 based SPCE sensor for isopropanol vapor, the sensing chip was exposed to different concentrations of isopropanol vapor (Table S1 in Supporting information), and the fluorescent sensitivity (F%) of the sensor to isopropanol vapor was defined as the percentage of the change in emission intensity (I) to the original intensity (I_0) when adsorbing isopropanol vapor (Eq. 1):

$$F = \frac{I}{I_0} \times 100\% \quad (1)$$

The response of the sensor to different concentrations of isopropanol vapor was illustrated in Fig. 4A. Due to the hydrophobicity of ZIF-8 [46], the sensor did not respond to water vapor (Fig. S10 in Supporting information). In contrast, the sensing film was responsive to isopropanol. Exposure of the sensing chip to vapors above different volume percentages of the isopropanol-water mix-

ture produced a concentration-dependent response to isopropanol vapor. The response of the sensor was saturated at high concentrations over 13,000 ppm (Fig. 4A and Fig. S11 in Supporting information). In the angle scanning SPCE method, the refractive index varied linearly with the SPCE angle (Fig. 4B and Fig. S12 in Supporting information). The refractive index of RhB@ZIF-8 film increased with the concentration of isopropanol vapor, implying that more isopropanol vapor with higher concentration was adsorbed into the pores of the RhB@ZIF-8 materials (Fig. 4C). At the same time, the fluorescence intensity (F_2) was enhanced due to the interaction between the isopropanol vapor and RhB molecules (Fig. 4D). The SPCE angle and fluorescence intensity synchronously changed in response to the adsorption of isopropanol vapor. The result showed that information on refractive index and fluorescence intensity obtained from the SPCE sensor can give coherent validation of the adsorption events of VOCs on the interface. With the SPCE sensor, the two events occurring during the adsorption of VOCs to the RhB@ZIF-8 materials could be measured simultaneously. Fig. 4D shows the signal intensity variation caused by refractive index change (F_1) and fluorescence intensity change (F_2) after adsorption of different concentrations of isopropanol vapor, and the intensity changes were measured at the angle of the maximum slope θ_{max}. Taking 9020 ppm of isopropanol as an example, the signal intensity variations caused by refractive index change (F_1) and the fluorescence intensity change of RhB@ZIF-8 (F_2) showed 158% and 263% of the original intensity, respectively. As a result, the SPCE signal (F_3) showed a 416% signal of the original intensity, which was the result of the parallel connection of the two signal intensity variations by the SPCE sensor.

In summary, we have developed a multi-information acquisition sensing strategy that can monitor simultaneously refractive index and fluorescence properties on the surface by a single fluorescence signal measurement. The dye@MOF based SPCE sensor was established with high sensing performance. The SPCE sensor monitored the changes of fluorescence property and refractive index of RhB@ZIF-8 simultaneously when adsorbing VOCs, and the SPCE sensor was able to amplify the response by parallelizing the signal variations caused by both. In the future, it is expected to introduce dielectric layers with different refractive index to achieve fluorescence encoding mediated by different emission angles or polarization. Cross-validation and complementation of multiple information can provide a reliable study on the interface. Achieving synchronicity in real time is essential for advancing the study of relevant chemical events on the interface. This all-in-one method offers new opportunities for monitoring chemical and physical phenomena on the interface including chemical sensing, biosensing, and nanotechnology.

Declaration of competing interest

The authors declared that they do not have any competing commercial or associative interests that could influence the work reported in this paper.

Acknowledgments

Financial support from the National Natural Science Foundation of China (Nos. 21874110, 21804098, 21974117 and 22274137) and the Science and Technology Program of Fujian Province (No. 2022Y4008) is gratefully acknowledged.

Supplementary materials

Supplementary material associated with this article can be found, in the online version, at doi:10.1016/j.cclet.2023.108181.

References

[1] J. Mei, N.L.C. Leung, R.T.K. Kwok, et al., Chem. Rev. 115 (2015) 11718–11940.
[2] J. Wu, B. Kwon, W. Liu, et al., Chem. Rev. 115 (2015) 7893–7943.
[3] Z. Yan, X. Lu, W. Du, et al., Nanotechnology 32 (2021) 465202.
[4] X. Wang, J. Zhu, Y. Xu, et al., Chin. Phys. B 30 (2021) 024207.
[5] J. Chen, Y. Kuang, P. Gu, et al., J. Lightwave Technol. 39 (2021) 4525–4528.
[6] J. Yu, P. Jia, S. Wang, et al., Sensor. Actuat. B: Chem. 321 (2020) 128469.
[7] L. Zhou, M.A. Arugula, B.A. Chin, et al., ACS Appl. Mater. Interfaces 10 (2018) 41763–41772.
[8] J.d.P. Rezende, E.A. Hudson, H.M. Campos de Paula, et al., Food Hydrocolloid 95 (2019) 526–532.
[9] V. Srinivasan, D. Vernekar, G. Jaiswal, et al., ACS Appl. Mater. Interfaces 8 (2016) 12324–12329.
[10] S.H. Cao, W.P. Cai, Q. Liu, et al., J. Am. Chem. Soc. 136 (2014) 6802–6805.
[11] N.H.T. Tran, K.T.L. Trinh, J.H. Lee, et al., Small 14 (2018) 1801385.
[12] K. Xie, S. Cao, Y. Zhai, et al., Chin. Chem. Lett. 30 (2019) 2173–2176.
[13] J.R. Lakowicz, Anal. Biochem. 324 (2004) 153–169.
[14] M. Chen, X.H. Pan, Q. Liu, et al., Anal. Chem. 91 (2019) 13658–13664.
[15] B. Rai, R. Malmberg, V. Srinivasan, et al., ACS Sens. 6 (2021) 4360–4368.
[16] J.S. Yuk, C. McDonagh, B.D. MacCraith, Anal. Bioanal. Chem. 398 (2010) 1947–1954.
[17] K.X. Xie, S.H. Cao, Z.C. Wang, et al., Sensor. Actuat. B: Chem. 253 (2017) 804–808.
[18] A. Rai, S. Bhaskar, K.M. Ganesh, et al., Mater. Chem. Phys. 285 (2022) 126129.
[19] A. Rai, S. Bhaskar, P. Battampara, et al., Mater. Lett. 316 (2022) 132025.
[20] S. Bhaskar, A. Rai, K.M. Ganesh, et al., Langmuir 38 (2022) 12035–12049.
[21] I. Nardi-Agmon, N. Peled, Lung Cancer 8 (2017) 31–38.
[22] Y. Shao, H. Chen, Y. Li, et al., Chem. Eng. J. 276 (2015) 51–58.
[23] Z. Jiang, X. Xu, Y. Ma, et al., Nature 586 (2020) 549–554.
[24] Z. Chen, P. Li, R. Anderson, et al., Science 368 (2020) 297–303.
[25] H. Zeng, M. Xie, T. Wang, et al., Nature 595 (2021) 542–548.
[26] Z. Ma, T. Yuan, Y. Fan, et al., Sensor. Actuat. B: Chem. 311 (2020) 127365.
[27] J. Wu, W. Zhang, Y. Wang, et al., Nanoscale 12 (2020) 9991–10000.
[28] M.A. Andres, M.T. Vijjapu, S.G. Surya, et al., ACS Appl. Mater. Interfaces 12 (2020) 4155–4162.
[29] M.J. Dong, M. Zhao, S. Ou, et al., Angew. Chem., Int. Ed. 53 (2014) 1575–1579.
[30] J.P. Zheng, S. Ou, M. Zhao, et al., Chempluschem 81 (2016) 758–763.
[31] J.F. Olorunyomi, M.M. Sadiq, M. Batten, et al., Adv. Opt. Mater. 8 (2020) 2000961.
[32] Y. Zhang, M. Gutierrez, A.K. Chaudhari, et al., ACS Appl. Mater. Interfaces 12 (2020) 37477–37488.
[33] L. Feng, C. Dong, M. Li, et al., Hazard. Mater. 388 (2020) 121816.
[34] C.Y. Liu, X.R. Chen, H.X. Chen, et al., J. Am. Chem. Soc. 142 (2020) 6690–6697.
[35] O. Dalstein, D.R. Ceratti, C. Boissiere, et al., Adv. Funct. Mater. 26 (2016) 81–90.
[36] W. Vandezande, K.P.F. Janssen, F. Delport, et al., Anal. Chem. 89 (2017) 4480–4487.
[37] A. Demessence, P. Horcajada, C. Serre, et al., Chem. Commun. 46 (2009) 7149–7151.
[38] Y.H. Weng, L.T. Xu, M. Chen, et al., ACS Macro Lett. 8 (2019) 223–227.
[39] H.N. Abdelhamid, Z. Huang, A.M. El-Zohry, et al., Inorg. Chem. 56 (2017) 9139–9146.
[40] K.S. Park, Z. Ni, A.P. Cote, et al., Proc. Nat. Acad. Sci. U. S. A. 103 (2006) 10186–10191.
[41] A. Colombelli, M.G. Manera, V. Borovkov, et al., Sensor. Actuat. B: Chem. 246 (2017) 1039–1048.
[42] L.T. Xu, M. Chen, Y.H. Weng, et al., Anal. Chem. 94 (2022) 6430–6435.
[43] B. Wiltschi, W. Knoll, E.K. Sinner, Methods 39 (2006) 134–146.
[44] S. Bhaskar, N.S. Visweswar Kambhampati, K.M. Ganesh, et al., ACS Appl. Mater. Interfaces 13 (2021) 17046–17061.
[45] S. Bhaskar, S.S. Ramamurthy, ACS Appl. Nano Mater. 2 (2019) 4613–4625.
[46] G. Lu, J.T. Hupp, J. Am. Chem. Soc. 132 (2010) 7832–7833.
[47] D. Roy, Appl. Spectrosc. 55 (2001) 1046–1052.